



Equilibrium and kinetic study of the adsorption of reactive blue, red, and yellow dyes onto activated carbon and barley husk

Abbas H. Sulaymon, Waleed M. Abood*

*Department of Environmental Engineering, College of Engineering, Baghdad University, Baghdad, Iraq
Tel. +964 07902279689; email: env_eng_waleed@yahoo.com*

Received 2 May 2012; Accepted 7 May 2013

ABSTRACT

Batch adsorption of reactive blue H3R (B), red 3BF (R), and yellow FG (Y) dyes onto activated carbon (AC) and barley husk (BH) was studied. Various experiments were carried out to find the effect of initial dye concentration (5–100 mg/l), adsorbent dosage (0.1–1 g), contact time (15–420 min), pH solution (2.5–8.5), and temperature 30°C. The experimental data showed that the increasing uptake at decreasing pH with respect to (AC) was with B and R dyes while in comparison with (BH) was showed increased uptake at pH increasing for all dyes. Adsorption capacity increased with increasing initial concentration of all dyes with (AC) and (BH). The experimental data were analyzed using Langmuir, Freundlich, and Sips isotherm models. The adsorption of B, R, and Y dyes with (AC) was well fitted with all above models with R^2 (0.925–1), while adsorption onto (BH) for B dye showed R^2 (0.87–0.96) for above models, while for other dyes showed low R^2 values. Pseudo-first-order, pseudo-second-order kinetic, and intraparticle diffusion models were used to analyze the kinetic data. The data were well fitted at dye concentration 10 ppm with the pseudo-first order when R^2 values for B, R, and Y dyes were (0.88, 0.97, and 0.982) and (0.98, 0.947, and 943) for (AC) and (BH), respectively, while intraparticle models with R^2 values were (0.97, 0.9, and 0.818) and (0.932, 0.8, and 0.947) for each of (AC) and (BH), respectively. Pseudo-second-order model showed well fitting for (AC), when R^2 values were (0.77, 0.965, and 0.998) for B, R, and Y dyes, respectively.

Keywords: Reactive dyes; Adsorption; Activated carbon; Barley husk

1. Introduction

Today, the main challenge for the textile industry is to modify production methods so that they are more ecologically friendly at a competitive price by using safer dyes and chemicals and by reducing cost of effluent treatment. There are three ways to reduce pollution; using new and less polluted technology,

effective treatment effluent so that it conforms the specified discharge requirement and recycling waste several times before discharge [1]. Characteristics of wastewater from textile processes can be high in BOD, alkalinity, total solids, temperature, acidity, and spent solvent [2]. The real hazard caused by color and solid in waste is dye toxicity and the ability to interfere with the transmission of light through water body and thus hindering photosynthesis in aquatic plants [3].

*Corresponding author.

Synthetic dyes have many structural varieties such as acidic, basic, and disperse or can be classified cationic, nonanionic, and anionic types. Anionic dyes include the direct and reactive dyes, nonionic dyes refer to disperse dyes that do not ionize in aqueous medium and cationic dyes refers to basic dyes [4]. Reactive dyes gained popularity in the twentieth century as dyes that give permanent coloration to celluloses textile substrates. Reactive dyes are soluble in water and are classified to many types according to their functional group which work as reactive group which react with fiber [5].

Textile dyeing may use azo-reactive dyes which are characterized by nitrogen to nitrogen double bond (N=N azo group) in their structure, when the color of azo group dyes is due to this bond associated with chromospheres. The dyes are first adsorbed onto cellulose and then react with the fiber. The reaction occurs by the formation of covalent bond between the dye molecule and the fiber which is much more resistant to unusual conditions of use. The reactive system of this kind of dyes reacts with ionized hydroxyl group (–OH) on cellulose. [6] Many reactive dyes (azo group) are toxic to some organisms and may cause direct destruction of aquatic life due to the presence of aromatic and metal chlorides. It has been reported that some azo dyes are able to produce carcinogenic aromatic amines due to high solubility which makes their removal a very difficult task [7].

Majority of dyes are visually detected even at concentrations less than 1 mg/l when the same dyes are either toxic or mutagenic and carcinogenic [8].

There are many technologies currently available for treating wastewater from textile industry which include biological treatment, chemical precipitation, adsorption, ultra-filtration and advanced oxidation [3].

The adsorption process is widely used and most-promising technique to produce effluent containing very low level of dissolved organic compounds but this application is limited by the high cost of adsorbent such as activated carbon [9]. There are many studies using cheap adsorbent like pear milled husk, date pits, saw dust, coir pith, crude oil residue, topical grass, olive stone, almond shell, pine bark, wool waste, and other carbonaceous precursors for the removal of dyes from wastewater [10]. Low-cost adsorbent was developed from tamarind fruit shell as agricultural waste or by-product for the removal of Congo red di-azo group dyes, with the possibility of recycling of the adsorbent after the adsorption process [11].

There is a number of analytical methods that may be used for the quantitative analysis of dyes solution

such as chemical oxygen demand to characterize the content of organics which can be oxidized to inorganic and visible absorption spectrophotometer method [12].

The aim of the present study is comparing the equilibrium and kinetic process of the adsorption of three reactive dyes *B*, *R*, and *Y* onto activated carbon or barley husk.

2. Adsorption isotherm models

The adsorption isotherm is an invaluable curve describing the phenomenon governing the retention or mobility of substance from the aqueous solution to a solid phase at constant temperature and pH. Adsorption equilibrium is established when adsorbate phase has been contacted with the adsorbent for a sufficient time. This is occurred where the adsorbate concentration in bulk solution in the dynamic balance with the interface concentration. Different mathematical models had been introduced to describe the adsorption isotherm model at equilibrium and were classified into: two parameter isotherms (e.g. Langmuir and Freundlich models), three parameter isotherms (e.g. Sips model) and multilayer-physisorption isotherms (e.g. Brunauer–Emmett–Teller BET model) [13].

2.1. Langmuir isotherm model

Langmuir isotherm is a theoretical isotherm model developed in 1916. This model is based on few assumptions; all sites are identical and equivalent, thermodynamically this implies that each site can hold one adsorbate molecule. Adsorption cannot proceed beyond monolayer; the ability of a molecule to be adsorbed at a given site is independent of the occupation of neighboring sites. This means there will be no interactions between adjacent molecules on the surface and immobile adsorption, that is, transmigration of the adsorbate in the plane of the surface is precluded (Table 1). The effect of the isotherm shape has been discussed with a view to predict whether an adsorption system is “favorable” or “unfavorable” proposed by a dimensionless separation factor, R_L Eq. (1). This is an essential feature of the Langmuir isotherm defined as. [9]:

$$R_L = \frac{1}{1 + K_L C_o} \quad (1)$$

Value of R_L indicates the shape of the isotherm according to:

Table 1
Nonlinear and linear form of adsorption isotherm models

Isotherm	Nonlinear form	Linear form
Langmuir	$q_e = \frac{q_m K_L C_e}{1 + K_L C_e}$	$\frac{C_e}{q_e} = \frac{1}{q_m K_L} + \frac{C_e}{q_m}$ ($\frac{C_e}{q_e}$ vs. C_e) $\frac{1}{q_e} = \frac{1}{q_m K_L C_e} + \frac{1}{q_m}$ ($\frac{1}{q_e}$ vs. $\frac{1}{C_e}$)
Freundlich	$q_e = K_F C_e^{1/n}$	$\log q_e = \log K_F + 1/n \log C_e$ ($\log q_e$ vs. $\log C_e$)
Sips	$q_e = \frac{(K_s q_m C_e)^{n_s}}{1 + (K_s C_e)^{n_s}}$	$n_s \ln C_e = -\ln \frac{K_s q_m}{q_e} + \ln K_s$ $\ln \left(\frac{K_s q_m}{q_e} \right)$ vs. $\ln(C_e)$ $\ln \left(\frac{K_s q_m}{q_e} \right)$ vs. $\ln(C_e)$

$0 < R_L < 1$ favorable, $R_L > 1$ unfavorable, $R_L = 1$ linear and $R_L = 0$ irreversible.

2.2. Freundlich isotherm model

Freundlich isotherm model is the earliest known relationship describing the nonideal and reversible adsorption, not restricted to the formation of monolayer. This empirical model can be applied to multilayer adsorption, with nonuniform distribution of adsorption heat and affinities over the heterogeneous surface (Table 1). The slope of Freundlich linear model (0–1) is a measure of the adsorption intensity or surface heterogeneity. It becomes more heterogeneous as its value gets closer to zero. Whereas a value below unity implies chemisorptions process, while (1/ n) above one is an indicative of cooperative adsorption [13].

2.3. Sips (Langmuir–Freundlich combination) isotherm model

Sips isotherm model is a combined form of Langmuir and Freundlich expression deduced for predicating the heterogeneous adsorption system and circumventing the limitation of the rising adsorb at concentration associated with Freundlich isotherm model. At low adsorbate concentrations, it is reduced to Freundlich isotherm, while at high concentration, it predicts a monolayer adsorption capacity characteristic of Langmuir isotherm. As a general rule, the parameters of the equations in Table 1 are governed mainly by the operating condition such as alteration pH, temperature, and concentration [13].

3. Adsorption kinetics

The prediction of batch sorption kinetics gives the most important information for designing batch sorption systems. The nature of sorption process will depend on the physical or chemical characteristics of the adsorbent system and also on the system conditions. In order to investigate the mechanism of sorption, characteristic constants of sorption can be determined using two simple kinetic models. The transient behavior of the dye sorption process and the potential rate-controlling steps involved in the sorption of dye were analyzed by using pseudo-first-order, pseudo-second-order kinetics and intraparticle models which have been used to fit experimental data at various dye concentrations [8] (Table 2).

3.1. Pseudo-first-order model

This model is expressed by changing the adsorption capacity with time. The pseudo-first-order rate suggested originally by Lagergren which is based on solid capacity is listed in Table 2.

3.2. Pseudo-second-order model

This model is expressed by changing of adsorption capacity (amount of adsorbed dye per mass of adsorbent) with time as listed in Table 2.

3.3. Intraparticle diffusion model

It is necessary to identify the steps involved during adsorption in order to interpret the mechanism of adsorption. It is assumed that the adsorption process

Table 2
Kinetic models

Kinetic model	Linear form
<i>Pseudo first order</i>	
$\frac{dq_t}{dt} = K_1(q_e - q_t)$	$\log(q_e - q_t) = \log q_e - \frac{K_1}{2.303}t$ $\log(q_e - q_t)$ vs. t
<i>Pseudo second order</i>	
$\frac{dq_t}{dt} = K_2(q_e - q_t)^2$	$\left(\frac{t}{q_t} = \frac{1}{K_2q_e^2} + \frac{t}{q_e}\right)$ $\frac{t}{q_t}$ vs. t
<i>Intraparticle diffusion</i>	
	$q_t = K_i t^{0.5} + I$ q_t vs. $t^{0.5}$

consists in several steps: migration of the dye from the bulk solution to the adsorbent surface, diffusion of the dye through the boundary layer, intraparticle diffusion, and adsorption of the dye on the internal adsorbent surface.

4. Experiments, methods, and materials

4.1. Materials

4.1.1. Adsorbents

Two types of adsorbent were used activated carbon and barley husk with specification shown in Table 3.

The following tests were carried out according to:

- Surface area analyses: BET method (surface area and porosity analyzer), ASAP 2020, by Micromeritics Co., USA.
- Void volume analyses: BET method (surface area analyzer, Qsurf M1, by Thermo Co., USA).

Table 3
Adsorbents specifications

specifications	AC	BH
Source	Provided by Unicarbo company Italy for local markets	Local Iraqi mills
Origin	Coco nut shell	Barely milling waste
Bulk density (real density) kg/m ³	711.8 (1,529)	203.1 (1,337)
Surface area m ² /g	911.581	0.2156
*Porosity %	53.44	84.809

- Bulk density (Auto top, by Quanta Chrome Co., USA).
- Real density (gas pycnometer, by PMI, USA. Using helium gas under vacuum pressure).

Activated carbon (AC) and Barley husk (BH) adsorbents had been washed by distilled water several times in order to remove dust and unwanted parts then dried using an electrical oven type (Heraeus, T 5042, W. Germany) for 12 h at temperature 100 and 60°C, respectively [8] and sieved for the desired size (0.5–0.75 mm).

4.1.2. Adsorbate

Simulated stock solutions for three reactive dyes (Blue B, Red R, and Yellow Y) had been prepared by dissolving 1 g of each dye in one liter distilled water and then diluted to get the desired concentration [14].

Table 4 shows the specification of these dyes. Knowing that some suppliers kept the specifications of their product as know how due to commercial reasons [15].

The chemical structures of reactive B and R dyes are shown in Fig. 1 [16–18].

UV-VIS absorption spectrophotometer method is used for the determination of the dye color concentration in their mixture.

The main principle of the quantitative UV-visible spectrophotometer technique is a linear relation between absorbance A and concentration of a dissolved sample C (mg/l) which is given by Beer-Lambert law Eq. (2) [19].

$$A = KC + E \quad (2)$$

Concentration of each dye was measured using double beams spectrophotometer (Labomed, UVD.3500,USA) and single-beam spectro photometer type (APEL PD- 303 UV JAPAN) [20].

4.2. Experiments and methods

The pH (2.5, 4.5, 6.5, and 8.5 ± 0.3) experiments were carried out by prepared samples of 10 ppm of each single dye (B, R and Y) by adding HCl and NaOH to achieve the desired pH. The pH of solution was measured by using a pH-meter type (Jenway, Model 3510, UK).

Adding 0.5 g of (AC) and (BH) individually to all samples and shaking by a shaker type (Infors HT, TMR, SWISS) at 200 rpm for 12 h, the results were plotted as uptake% [Eq. (3)] vs. pH [8].

Table 4
Specification of dyes

Item	Reactive blue	Reactive Red	Reactive Yellow
Trade name	Blue H3R	Red 3B	Yellow FG
Origin	India	China	Swiss
Phase	Solid/ Powder Package 25 kg	Solid/ Powder Package 25 kg	Solid/ Powder Package 25 kg
Wave length(nm)	585	540	420
Solubility g/l	90	100	150

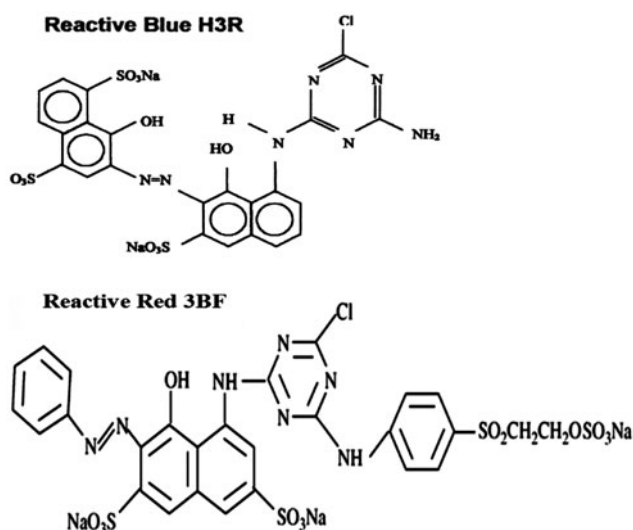


Fig. 1. Chemical structure of Red and Blue dyes.

$$\text{Uptake \%} = \frac{C_0 - C_e}{C_0} \% \quad (3)$$

To show the effect of the initial concentration (5, 10, 25, 40, 50, 75, and 100 mg/l) on uptake% or adsorption capacity (q_e), Eq. (4) was used to find the adsorbent dosage to prepare seven solutions of 100 ml for each single dye (B, R and Y), 0.5 g of adsorbent added to each samples and shaken at 200 rpm for 12 h. The results were plotted as the relation between the adsorption capacity q_e vs. initial concentration C_0 Eq. (4).

The uptake% vs. adsorbent dosage was plotted to evaluate the type of curve comparing with the standards isotherm models (Table 1).

$$q_e = \frac{(C_0 - C_e)V}{m} \quad (4)$$

Adsorption equilibrium experiments were carried out using different adsorbent (AC, BH) dosage (0.1, 0.2, 0.3, ... 1) g for 10 samples (100 ml solution) of single dye (B, R and Y) with (C_0) 10 ppm placed in

300 ml glass containers at $\text{pH } 6.5 \pm 0.3$ and temperature $30 \pm 3^\circ\text{C}$ and shaken at speed 200 rpm for 12 h.

For kinetic study, twelve samples with (100 ml) of each dye solution had been contacted with 0.5 g of adsorbents (AC, BH) individually at $\text{pH } 6.5 \pm 0.5$ and temperature $30 \pm 5^\circ\text{C}$ and agitated at 200 rpm. At desired interval times, (15, 30, 60, 120 ... 420) min, samples were analyzed to determine the amount of adsorbed dye per mass of adsorbent q_t at time t Eq. (4).

The results (q_t vs. t) were plotted and from kinetic relations Table 2, the type of mass transfer mechanism (external, internal mass transfer, or/and intraparticle diffusion) can be derived [21].

All above samples were filtrated before analyses using filter paper, the first part of the filtrated liquor was discarded to eliminate the effect of the adsorption on the filter media [22].

5. Results and discussions

5.1. Effect of pH

Fig. 2 shows the decrease in $\text{pH} < 7$ (i.e. increasing H^+ ion) which led to increase adsorbed dye uptake %. The uptake% decreases with increasing $\text{pH} > 7$ (i.e. increasing OH^- ion). This is due to the net surface charge on the surface of AC which is positive due to adsorption of excess H^+ ion, which favors adsorption of anion due to Columbic attraction. At $\text{pH} > 7$ the net surface charge is negative due to desorption of H^+ and adsorption must compete with Columbic repulsion. The consistent dye removal in the pH range 2.5–5, could be due to the combined effect of both chemical and electrostatic interactions between protonated adsorbent surfaces and SO_3^- ion in the dye. The observed reduction in dye adsorption at pH 6–7 may suggest that the strong negative surface charge developed may cause repulsion for the available adsorption sites. Another factor is that in alkaline medium, lower adsorption capacity may be due to the competition of OH^- ions with dye anions. The decrease in dye adsorption is particularly sharp above pH 7, as the surface

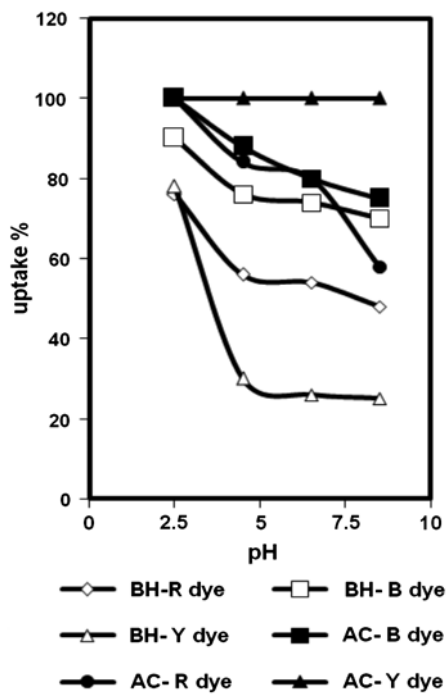


Fig. 2. pH effect on dye uptake.

charge becomes more negative. Hence, dye ions would have to overcome electrostatic forces as there would be a higher density of negative charge very close to the surface, hence greater electrostatic repulsion. The results are in harmony with [23,24].

This phenomenon is an exception for Y dye which is classified as an vinyl sulfone type which tends to longer lasting in water due to its high solubility and the result shows the adsorption can be considered mainly physical adsorption with AC and no chemical reaction which cause the binding as shown later more than BH adsorbent which agrees with adsorption of yellow reactive dyes [25].

5.2. Effect of initial dye concentration

Fig. 3(a)–(c) show changing dye concentrations (5, 10, 25, 40, 50, 75, and 100 mg/l) which have clear effect on the adsorption capacity of AC or BH, and small effect for BH at high concentrations of the Y dye (Fig. 3(c)).

There are changes in the behavior of curve of B and R dyes, due to increase in initial concentration which plays the role of a driving force which enhances the process of mass transfer, but in the case of BH low surface area and nonporous material lead to formation of aggregate of the dye on the adsorbent particles [26].

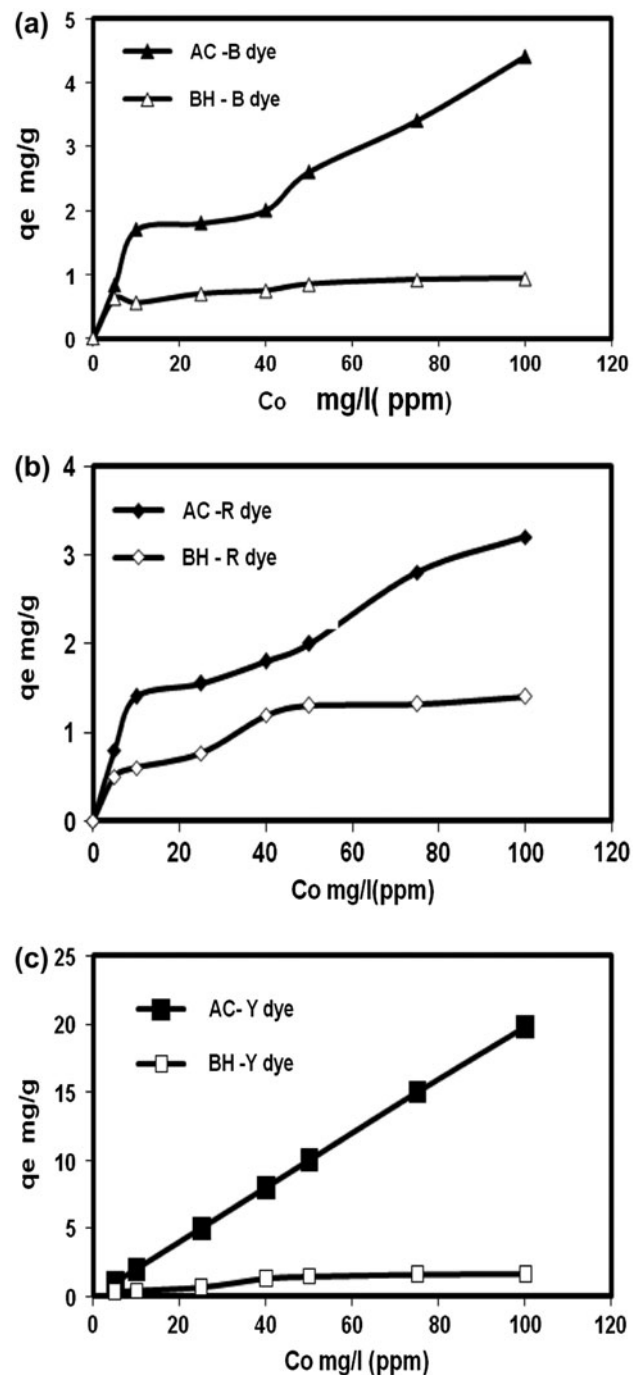


Fig. 3. Effect of initial dye concentration on the adsorption capacity.

5.3. Effect of adsorbent dose

Fig. 4 shows that for each adsorbent and dye solution, there is an increase in the adsorbent dosage from 0.1 to 1 g resulting in an increase in the amount of adsorbed dye, that is, the increase in removal was due to the availability of sites on the adsorbent surface to adsorb dye molecules [27].

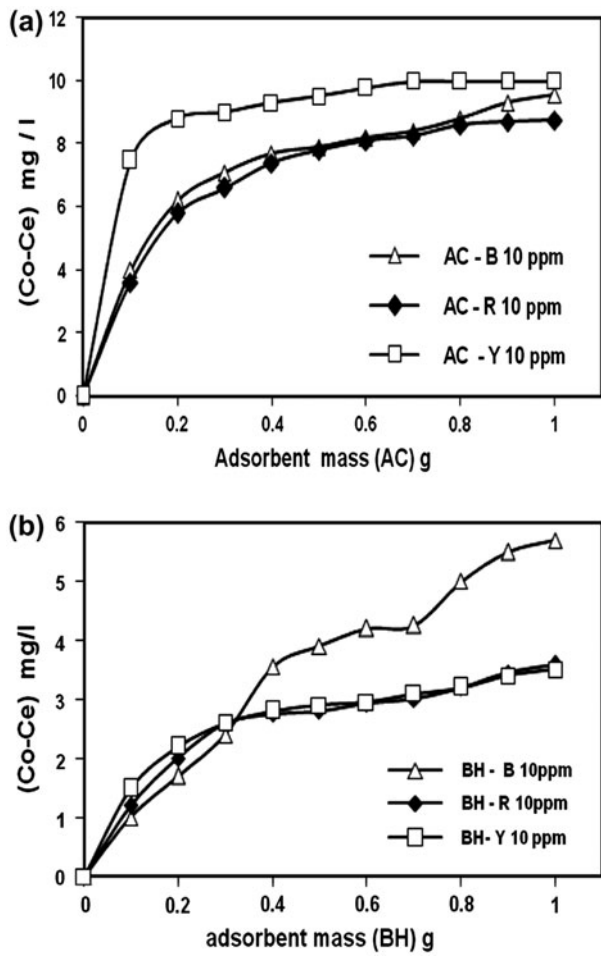


Fig. 4. Effect of adsorbent dose.

The adsorbent dosage is represented by an important parameter due to its strong effect on the capacity of an adsorbent at a given initial concentration of adsorbate.

The increase in the adsorption capacity was found to be steeper at low dosages. Many factors can contribute to this effect. The most important factor is that adsorption sites remain unsaturated during the adsorption reaction.

Examining the results of Fig. 4 and using Eq. (4) to calculate q_e for fitting the experimental data with the equilibrium isotherm models Table 1, the model constants were found as shown in Table 5.

From Table 5, it can be seen that the adsorption onto AC can fit well Langmuir, Freundlich and Sips models for all single dyes with R^2 (0.925–1), while adsorption onto BH for B dye shows R^2 (0.87–0.96) for all models with a low value for R dye and unacceptable for Y dye. This may be due to high solubility of this dye which leads to less ability of adsorption for low surface area material, and effect of repulsive force between adsorbent surface and anionic dyes [8].

Table 5
Constants of equilibrium isotherm models

Isotherm	AC			BH		
	B	R	Y	B	R	Y
<i>Langmuir</i>						
q_m	10.56	12.6	28.25	2.605	24.24	23.8
K_L	0.187	0.062	0.1406	0.064	0.009	0.004
R_L	0.348	0.617	0.415	0.61	0.917	0.961
R^2	0.95	0.95	0.975	0.91	0.37	0.28
<i>Freundlich</i>						
K_F	0.965	0.807	0.788	0.204	0.0005	0.0094
n	1.238	1.2	1.6	1.4	0.27	0.33
R^2	0.96	0.97	1	0.87	0.85	0.77
<i>Sips</i>						
q_m	26.46	6.96	23.97	2.57	3.06	3.83
K_s	0.037	0.11	0.015	0.064	0.0007	0.00326
n_s	1.13	0.81	1.2	1	0.3	0.34
R^2	0.95	0.94	0.925	0.96	0.7	0.6

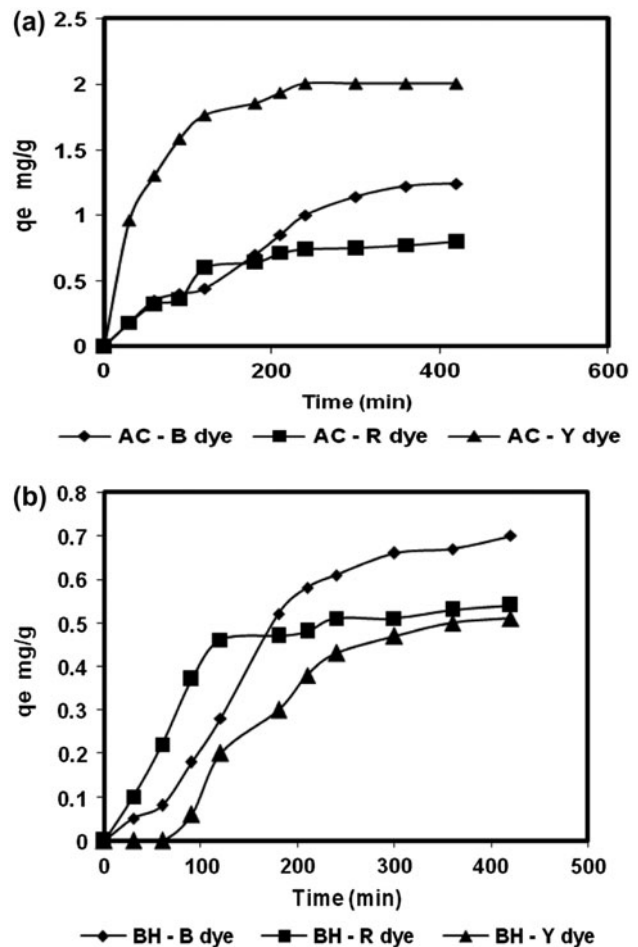


Fig. 5. Effect of contact time at adsorption capacity.

Table 6
Constants of kinetic models

Kinetic model	AC			BH		
	B	R	Y	B	R	Y
q_{exp} (mg/g)	1.24	0.8	2	0.7	0.54	0.51
<i>Pseudo first order</i>						
q_{cal} (mg/g)	2.36	0.8	1.57	1.148	0.48	1.1
K_1 (1/min)	0.011	0.01	0.0143	0.0103	0.0106	0.0115
R^2	0.88	0.97	0.982	0.98	0.947	0.943
<i>Pseudo second order</i>						
q_{cal} (mg/g)	2.85	1.1	2.2	−19.8	0.76	−0.6
K_2 (g/mg min)	0.0007	0.0065	0.013	0.000044	0.01	0.0025
R^2	0.77	0.965	0.998	0.2	0.9	0.22
<i>Intraparticle diffusion</i>						
K_i (mg/g min) ^{0.5}	0.0786	0.013	0.0655	0.05	0.0267	0.0407
R^2	0.97	0.9	0.818	0.932	0.8	0.947

R_L values were in the range of 0.348–0.617 for AC which was referring to favorable isotherm, and for BH the range was 0.61–0.961 which is favorable for B dye and near to linearly for R and Y dyes [28].

5.4. Effect of contact time

Adsorption capacity q_t was found at interval times t using Eq. (4) for each dye (10 ppm). Plots of q_t vs. t for adsorbent dosage of AC and BH are shown in Fig. 5(a),(b), respectively. It can be seen that q_t increases with increasing time and it reaches steady state at 300–350 min.

Utilizing the results of Fig. 5(a),(b) and Eq. (4), q_t and accumulation (q_{exp}) are calculated. Applying kinetic models to examine fitting these results with models, q_{cal} , values are listed in Table 6. Examining the results in Table 6, it can be seen that fitting with the pseudo first order model with R^2 for AC and BH adsorbents for B, R and Y dyes are 0.88, 0.97 and 0.982 and 0.98, 0.947 and 0.943, respectively.

R^2 values for the pseudo-second order for AC with R and Y dyes are 0.965 and 0.998, respectively, and for BH with R dye (0.9). Intraparticle model shows R^2 for AC and BH at B, R and Y dyes are 0.97, 0.9 and 0.818 and 0.932, 0.8 and 0.947, respectively.

6. Conclusion

- Activated carbon or barley husk uptake for reactive blue, red, and yellow dyes increase at low pH (<6).
- Initial concentration plays an effective role as a driving force of increasing adsorption capacity of

AC at all concentration and BH at low concentration due to availability of active sites.

- Good fittings were obtained with Langmuir, Freundlich and Sips isotherm models for adsorption of all reactive dyes with AC, while with BH reactive blue dye only shows good fitting with these models, as R_L values refer to a favorable isotherms.
- Experimental results show good fitting with Pseudo-first-order model shows for AC and BH with R^2 for B, R, and Y dyes are 0.88, 0.97, and 0.982 and 0.98, 0.947, and 0.943, respectively, followed by intraparticle diffusion model of AC and BH with R^2 values for B, R and Y dyes of 0.97, 0.9, and 0.818 and 0.932, 0.8, and 0.947, respectively.

Symbols

- A — absorbance spectrophotometer of given dye at its wavelength λ
- C — dye concentration in solution (mg/l)
- C_e — equilibrium dye concentration in solution (mg/l)
- C_o — initial dye concentration in solution (mg/l)
- C_t — dye concentration in the solution at interval time t (mg/l)
- E — intercept of the linear relation of a dye and its absorbance in standard curves
- K — absorbance coefficient of linear relation of dye and its absorbance in standard curves
- K_1 — the rate constant for the first-order kinetics (1/min)
- K_2 — the rate constant for the second-order kinetics (g/mg min)

- K_F — Freundlich constant indicating adsorption capacity (mg/g)
- K_L — Langmuir constant related to the affinity of the binding sites (l/mg)
- K_s — Sips model constant (l/mg)
- m — mass of adsorbent (g)
- n — Freundlich constant indicating to adsorption intensity
- q_{cal} — calculated of the amounts of adsorbed dye per unit weight of adsorbent by kinetic pseudo models (mg/g)
- q_e — the amounts of adsorbed dye per unit weight of adsorbent at equilibrium (mg/g)
- q_{exp} — accumulated adsorption capacity in kinetic experiments (mg/g)
- q_m — maximum adsorption capacity of the dye (forming a monolayer) per unit weight of adsorbent (mg/g)
- q_t — the amounts of adsorbed dye per unit weight of adsorbent at interval time (mg/g)
- R_L — dimensionless factor Indicating the nature of the adsorption process
- t — interval time of sampling min
- V — volume of sample in experiments (ml)

References

- [1] B.R. Babu, A.K. Prande, S. Raghu, T.P. Kumar, Cotton textile processing: Waste generation and effluent treatment, *J. Cotton Sci.* 11 (2007) 141–153.
- [2] N.L. Nemerow, *Industrial Water Pollution-Origins, Characteristics and Treatment*, Addison-Wesley, Canada, 1971.
- [3] T.R. Demmin, *Improving Carpet Waste Water Treatment*, American Dyestuff Reporter, New York, 1988.
- [4] K.N. Tapley, *Reactive Dyes*, Kaliakor Dye Managers Workshop, University of Leeds, UK, September, 2003.
- [5] Z. Mbolekwa, Removal of reactive dyes from dye liquor using activated carbon, M.Sc. thesis, University of Kwazulu-Natal, Durban, 2007.
- [6] Y.S. Al-Degs, S. Allen, M.N. Ahmed, Effect of carbon surface chemistry on the removal of reactive dyes from textile effluent, *Water Res.* 34 (2000) 927–935.
- [7] A.S. Mahmoud, A.E. Ghaly, M. Brooks, Removal of dye from textile wastewater using plant oils under different pH and temperature conditions, *Am. J. Environ. Sci.* 3 (2007) 205–218.
- [8] S.T. Ong, P.S. Keng, C.K. Lee, Basic and reactive dyes sorption by modified rice hull, *Am. J. Appl. Sci.* 7 (2010) 447–452.
- [9] Z. Zawani, C.A. Luqman, S. Thomas, Equilibrium, kinetic and thermodynamic studies adsorption of remazol black 5 on the palm kernel shell activated carbon, *Eur. J. Sci. Res.* 37 (2009) 67–76.
- [10] M. Hema, S. Arivoli, Comparative study on the adsorption kinetic and thermodynamics of dyes onto acid activated low cost carbon, *Int. J. Phys. Sci.* 2 (2007) 10–17.
- [11] M.C. Reddy, Removal of direct dye from aqueous solution with an adsorbent made from an agricultural solid waste, *J. Sci. Ind. Res.* 65 (2006) 443–446.
- [12] E. Ekrami, M. Okazi, Analysis of dye concentration in binary dye solution using derivative spectrophotometric techniques, *World Appl. Sci. J.* 11 (2010) 1025–1034.
- [13] K.Y. Foo, B.H. Ahmed, Insight into the modeling of adsorption isotherm systems, *Chem. Eng. J.* 156 (2010) 2–10.
- [14] Y.S.M. Al-Degs, M.A. Khraisheh, S.J. Allen, M. Ahmed, Adsorption characteristics of reactive dyes in column of activated carbon, *J. Hazard. Mater.* 165 (2009) 944–949.
- [15] M.A. Al-Gouti, M.A. Khraisheh, S.J. Allen, M. Ahmed, Adsorption of heavy metals ions onto modified diatomite, *J. Hazard. Mater.* 146 (2007) 316–327.
- [16] B. Manu, B.M. Chaudhari, Decolorization of indigo and azo dyes in semi continuous reactors, *J. Process Biochem.* 38 (2003) 1213–1221.
- [17] M. Rachakornlij, S. Ruangch, S. Teachakul, Removal of reactive dyes from aqueous solution using bagasse fly ash, *J. Sci. Technol. Thailand* 26 (2004) 13–24.
- [18] M. Chaudhuri, E.S. Elmolla, R. Othman, Removal of reactive dyes from aqueous solution by adsorption coconut coir activated carbon, 2nd International Conference on Engineering Technology (ICET 2009), Kuala Lumpur, December 2009.
- [19] Y.S. Al-Degs, M.A. Khraisheh, S.J. Allen, M. Ahmed, G.M. Walker, Competitive adsorption of reactive dyes from solution: Equilibrium isotherm studies in single and multisolute systems, *Chem. Eng. J.* 128 (2007) 163–167.
- [20] O. Karmo, Adsorption the dyes from effluent of textile factories by activated carbon, *J. Eng. Sci. Al-Assad University of Damascus*, 23 (2007).
- [21] G. Annadurai, Adsorption of basic dye on strongly chelating polymer: Batch kinetic studies, *Iran. Polym. J.* 11 (2002) 237–244.
- [22] V.J. Poots, G. McKay, J. Healy, The removal of acid dye from effluent using natural adsorbents, *Water Res.* 10 (1976) 1061–1066.
- [23] R. Gong, X. Liu, M. Feng, N. Li, Comparative study of methylene blue on crude and monosodium glutamate functionalized sawdust, *J. Health Sci.* 54 (2008) 623–628.
- [24] S.T. Akar, T. Akar, A. Cabuk, Decolorization of textile dye reactive red 198 by fungal biosorbent, *Braz. J. Chem. Eng.* 26 (2009) 399–405.
- [25] R.F. Moreira, M.G. Peruch, N.C. Kuhnen, Adsorption of textile dye on alumina: Equilibrium studies and contact time effects, *Braz. J. Chem. Eng.* 49 (1998) 2313–2322.
- [26] M.M. Abdul El-Latif, A.M. Ibrahim, M.F. Kady, M.E. Ossman, Removal of methylene blue from aqueous solution in a batch stirred tank reactor, *J. Am. Sci.* 6 (2010) 280–292.
- [27] M.A. Mumin, M.M. Khan, M.J. Uddin, Potential of open burnt clay as an adsorbent of congo red from aqueous solution, *Int. J. Environ. Sci. Technol.* 4 (2007) 525–532.
- [28] V. Ponnusami, S. Vikram, Novel adsorbent for removal of methylene blue from aqueous solution, *J. Hazard. Mater.* 152 (2008) 276–286.